AXONAL TRANSPORT OF PROTEINS

A New View Using In Vivo Covalent Labeling

DAVID J. FINK and HAROLD GAINER

From the Section on Functional Neurochemistry, Laboratory of Developmental Neurobiology, National Institute of Child Health and Human Development, National Institutes of Health, Bethesda, Maryland 20205

ABSTRACT

The injection of [2,3-^{3}H]*N*-succinimidyl propionate ([^{3}H]*N*-SP) into the rat sciatic nerve was used to covalently label both intra- and extra-axonal proteins. While extra-axonal proteins (e.g., myelin proteins) remained in the injection site, the intra-axonal proteins were transported in both the anterograde and retrograde directions. The mobile labeled proteins appeared to move by normal axonal transport processes because: (*a*) autoradiographic studies showed that they were localized exclusively within the axon at considerable distances from the injection site, (*b*) specific and identifiable proteins (by SDS gel electrophoresis) moved at expected rates in the anterograde direction, and (*c*) an entirely different profile of proteins moved in the anterograde vs. retrograde direction. This novel experimental approach to axonal transport, which is independent of *de novo* protein synthesis, provided a unique view of slow anterograde transport, and particularly of retrograde transport of endogenous proteins. A large quantity of a 68,000 mol wt protein, moving at ~3–6 mm/day, dominated the retograde transport profile. [^{3}H]*N*-SP, therefore, represents a new and unique "vital stain" which may find many applications in cell biology.

The intra-axonal transport of proteins serves as an experimental window on the macromolecular organization of the neuron. After pulse labeling of the perikaryon with radioactive amino acids, labeled proteins are transported proximodistally in the axon (17, 18, 29, 37). This experimental paradigm has provided important information about the multiple rates of anterograde axonal transport and the specific constellations of proteins that are associated with each rate class (22, 30, 49, 51). In some cases, identification of the proteins in a given rate class has provided insight into the structural organization of the axon (19, 22, 30, 36).

However, axonal transport is not a unidirectional process. Direct visual observation of axons in vitro shows bidirectional and discontinuous movements of organelles (8, 11, 26, 45). Various studies employing axonal ligatures (1, 13, 15, 21, 25, 26, 28, 38) have suggested that a large number of proteins are capable of bidirectional transport. In addition, studies of the distribution of enzyme activity, particularly with the use of localized, transient, cold blocks to stop axonal transport, suggest that only a fraction of the axonal components may be undergoing translocation at any time (5, 6, 47). Although the pulse-labeling paradigm discussed above provides a unique view of the dynamics of anterograde axonal transport, there are severe limitations on its use in studies of retrograde transport. The pulse-labeling paradigm

depends on *de novo* protein synthesis which occurs only in the perikaryon of the neuron. Therefore, although transport of labeled proteins from the cell body can be studied in detail, the reverse transport from nerve terminals towards the cell body in intact (nonligatured) axons cannot be studied by this method. Hence, if one could label intra-axonal proteins by another means, at any topographical site in the neuron, one could follow bidirectional transport from the labeled site.

We have recently found that labeled *N*-acylsuccinimides can be used for this purpose. These acylating agents rapidly react at physiological pH, with free α- and ϵ-NH_2 groups of proteins (3, 31). Of greater importance, they rapidly permeate cell membranes and, hence, can be applied extracellularly to label intracellular proteins with no discernible effects on the viability of the cells. The covalent label is soluble in both aqueous and hydrophobic environments and, hence, both membrane and soluble proteins are labeled in the cells.

In this paper, we describe experiments in which [^{3}H]*N*-succinimidyl propionate ([^{3}H]*N*-SP) was locally injected into the rat sciatic nerve to covalently label intra-axonal proteins. These data demonstrate bidirectional transport of proteins from the injection site. Slow transport in the retrograde direction consists primarily of 68,000 mol wt protein. This novel paradigm also provides new insights into the dynamics of anterograde transport.

MATERIALS AND METHODS

Preparation of the Covalent Label for Injection

[^{3}H]*N*-SP in toluene was obtained from Amersham Corp. (Arlington Heights, Ill.) with a sp act of 50 Ci/mmol. *N*-SP is an activated ester which reacts with the free α-NH_2 group at the N-terminal of proteins, peptides, or amino acids, as well as the epsilon amino group of lysine in proteins to form an N-acyl bond (Fig. 1) (3, 31). The acylating agent reacts rapidly (half-time is 2–3 min) with substrates at physiological pH and slowly (half-time ~90 min) hydrolyzes in aqueous solutions to an inactive form in the absence of substrate. Therefore, to minimize the latter hydrolysis, the reagent in toluene is concentrated to a small volume (~10 μl) by a stream of nitrogen, and shortly before use this volume of toluene is added to the physiological saline to be injected. The residual toluene is then removed from the saline by a stream of nitrogen.

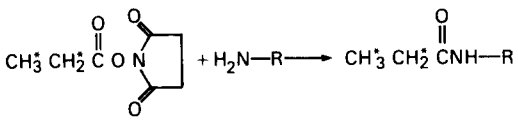

FIGURE 1 N-terminal acylation. *N*-succinimidyl propionate reacts with free N-terminal amino groups or the epsilon amino groups of lysine to form a stable N-acyl bond.

Animals and Operative Procedures

All experiments were performed on female Sprague-Dawley rats, 350–400 g. Under light ether anesthesia, the sciatic nerve of the rats was exposed. 1 μl of saline containing 100 μCi of [^{3}H]*N*-SP was injected into the nerve over 5 min, with a 29-gauge stainless steel hypodermic needle attached to a Harvard infusion pump (Harvard Apparatus Co., Inc., Millis, Mass.). The injection was underneath the nerve sheath, in the section of nerve below the branch to the gluteal muscle, but above the division into the muscles of the leg. At that point the nerve is unbranched for ~30 mm. After injection, the incision was closed by sutures, and the animal was allowed to recover from anesthesia. At various times after the injection, the animal was killed by decapitation, and the nerve from the spinal cord to the leg branches was removed en bloc and frozen on dry ice. The nerve was cut into 3-mm segments which were homogenized in 2 ml of 0.1 M HCl. Aliquots were removed for determination of TCA-precipitable radioactivity by conventional filter-pad procedures.

Gel Electrophoresis Procedures

The HCl homogenate was precipitated with 10% TCA. The precipitate was washed twice with acetone and twice with ether to remove the TCA, and suspended in 10 M urea containing 1% SDS, 5% BME, and 0.05 M Na_2CO_3. The proteins were separated on 11% polyacrylamide gels in SDS by use of the buffer system described by Neville (35). The gels were stained and destained by conventional procedures and sliced at 1.5-mm intervals. Slices were solubilized in appropriate cocktail and counted in a liquid scintillation counter. Slab gels were fluorographed by the method of Bonner and Laskey (2).

Autoradiography

Animals were injected as described above. At various times after injection, the animal was killed by decapitation. The nerve was removed and placed in 10% formalin. It was embedded in paraffin and sliced into 7-μm sections. Deparaffinized sections were coated with Kodak NTB2, diluted 1:1, dried upright, and stored at 4°C in light-tight boxes for 7 d. Radioautograms were developed in Kodak Dektol diluted 1:1 for 3 min at 16°C, fixed, washed, and stained with 0.1% sodium borate.

RESULTS

[^{3}H]N-SP Labels Mobile, Intracellular Proteins in the Sciatic Nerve

Immediately after the injection of [^{3}H]*N*-SP in the 1 μl of saline into the sciatic nerve, virtually all of the TCA-precipitable radioactivity is confined to the 3-mm segment containing the injection site (Fig. 2, dotted line). The amount of TCA-precipitable radioactivity falls off exponentially in both directions from the injection site (i.e., retrograde towards the cell body as well as anterograde towards the terminal region). Background levels

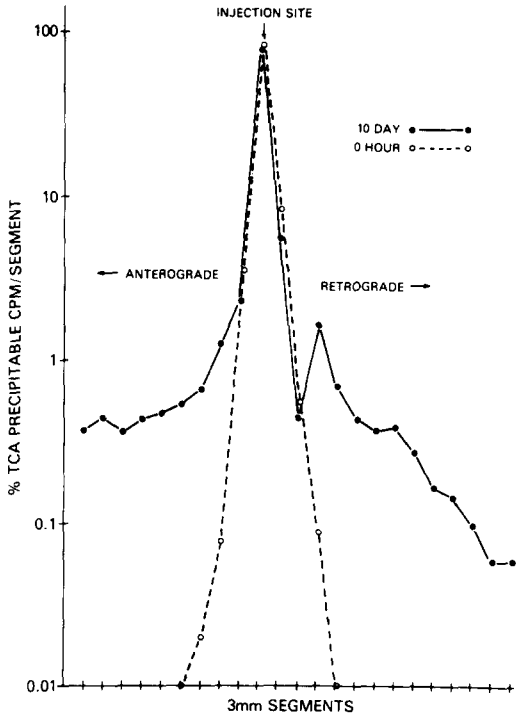

FIGURE 2 Pattern of TCA-precipitable radioactivity in the sciatic nerve after injection of [^{3}H]*N*-SP. At 15 min (- - -) and 10 days (–) after injection of the isotope, the sciatic nerve was removed and cut into 3-mm segments. The amount of TCA-precipitable radioactivity in each segment was determined. The amount in each segment is calculated as a percentage of the total number of counts in the nerve and graphed on a semi-log scale.

(similar to those obtained in 3-mm segments of either the contralateral sciatic nerve or ipsilateral femoral nerve) were found at distances >9 mm from the injection site.

In contrast, at 5 and 10 d after injections, segments up to 30 mm from the injection site contained significant amounts of TCA-precipitable radioactivity (Fig. 2, solid line, 10-d data shown). After 10 d, there was >10,000 cpm/3-mm segment, 30 mm from the injection site in both the retrograde and anterograde directions. The precise pattern of the distribution of TCA-precipitable radioactivity was variable in different injected animals. In most cases there were extended plateaus of radioactivity (e.g., as in Fig. 2, solid line). In some cases the counts fell continuously from the injection site with only a small plateau region. In no cases, however, were there any prominent peaks of radioactivity in the anterograde direction which correspond to the transport waves seen when pulse-labeling of the cell body is done (29, 37).

In the retrograde direction the counts fell exponentially at early times (15 min to 1 h). At times between 1 and 4 d, a prominent plateau usually extended ~18–24 mm from the injection site, and in general contained 10 times the radioactivity found in comparable segments in the anterograde direction. A discrete peak of radioactivity was not observed in the retrograde direction. Although quantitation at various times in different animals was difficult because of the variability of the injection procedure, it appeared that the amount of TCA-precipitable radioactivity in the retrograde direction tended to decrease with time. Although radioactivity moved in the retrograde direction for ~2–4 d, the retrogradely transported proteins in this relatively slow-moving component did not appear to move all the way back to the cell body.

The above data (Fig. 2) show that injection of [^{3}H]*N*-SP into the sciatic nerve effectively labeled proteins at that site, and that a significant fraction of these labeled proteins appeared to migrate in both directions along the nerve over time. The location of the labeled protein within the nerve was determined by autoradiography. A low magnification view (Fig. 3*A*) of the injection site and adjacent nerve in the anterograde direction after 5 d shows that at the injection site (asterisk, Fig. 3*A*) all of the cellular and extracellular elements are indiscriminately labeled. However, extending from the injection site, the label appears to be confined to a linear pattern that is axonal. Higher magnification views of other 5- and 10-d nerves at various distances from the injection site are shown in Fig. 3 *B–D*. Neither myelin, Schwann cells (nuclei) nor blood vessels are significantly labeled. Cross-sectional and longitudinal views confirm that the radioactive proteins were indeed intra-axonal (Fig. 3 *B–D*). These patterns of labeling were identical both anterograde to and retrograde from the injection site. They were likewise indistinguishable at 5 and 10 d. That is, the injection site was always diffusely labeled, whereas the silver grains outside the injection site were restricted to the axon interior.

The quantitative distribution along the nerve (Fig. 2) and the autoradiographic data (Fig. 3) indicate that while the [^{3}H]*N*-SP covalently attaches to proteins randomly at the injection site, a considerable amount is attached to mobile intracellular proteins within the axon. Is the subsequent movement of these intra-axonal proteins caused by axonal transport mechanisms or simply diffu-

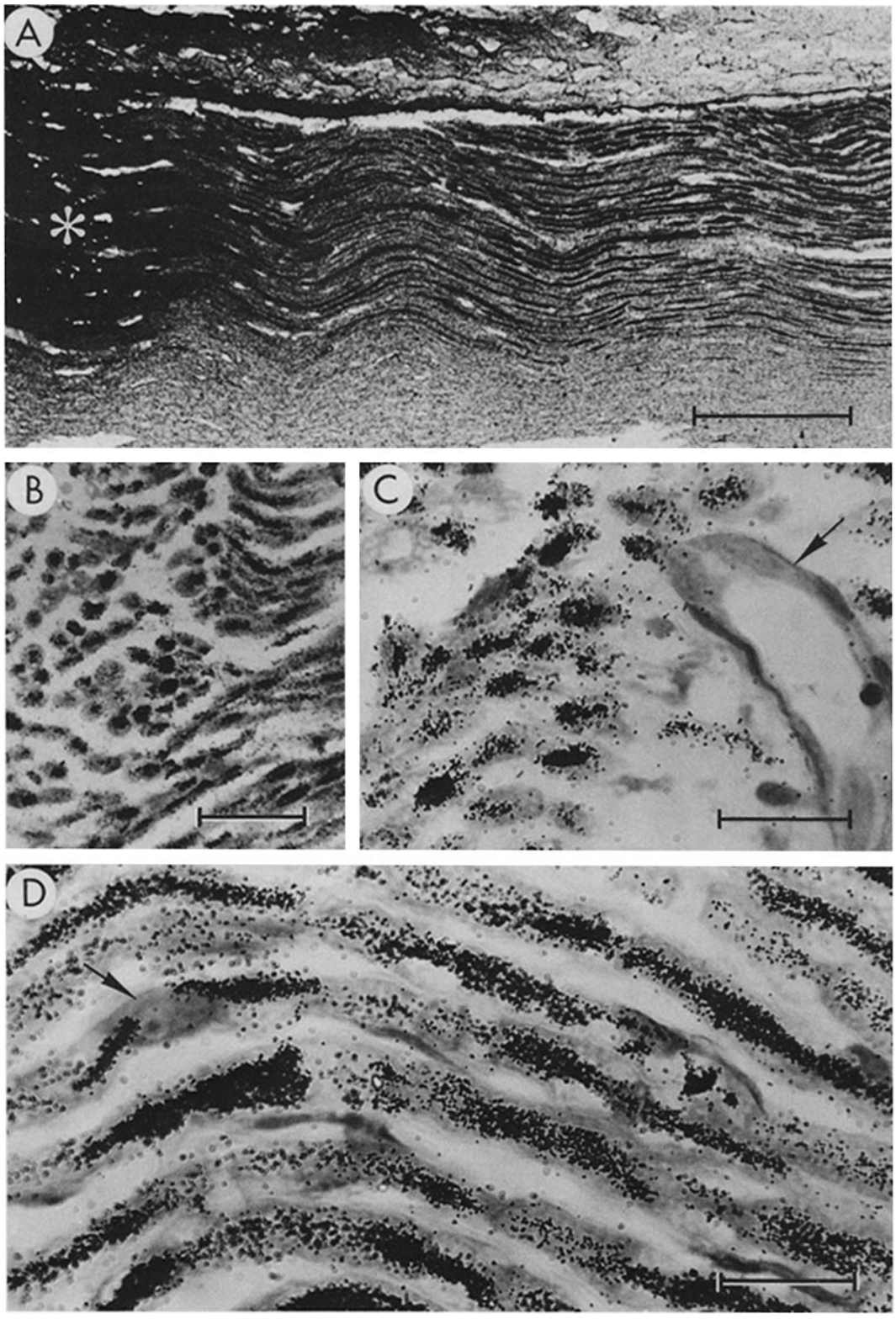
A
B
C
D

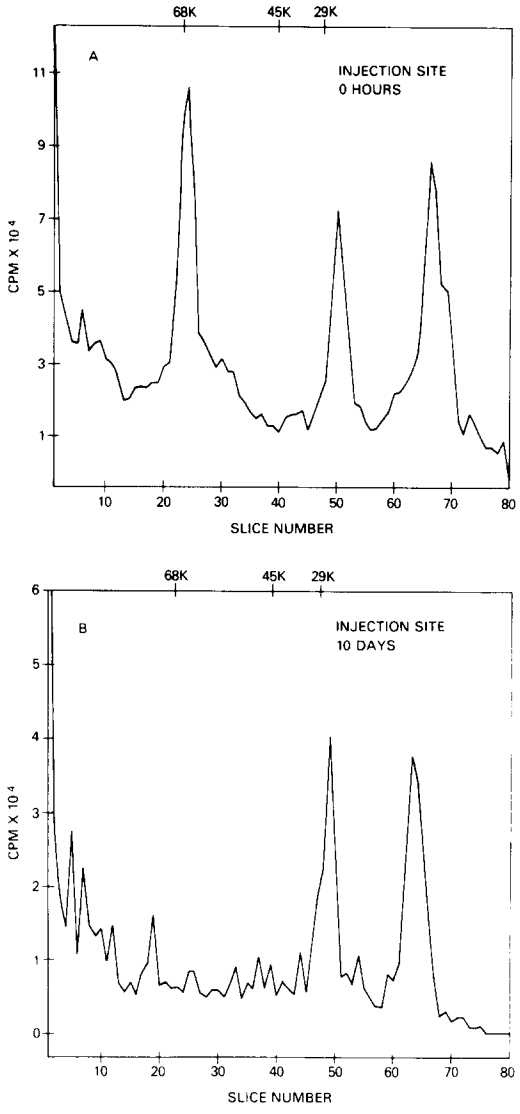

FIGURE 4 SDS PAGE of injection site. TCA-precipitable label from the 3-mm segment including the injection site was run on SDS polyacrylamide gels. The gels were sliced into 1.5-mm segments, and the segments were solubilized and counted in a liquid scintillation counter. Standards indicated on the upper abscissa were bovine serum albumin (68,000), ovalbumin (45,000), and carbonic anhydrase (29,000). (*A*) 15 min after injection. Three prominent peaks are identifiable at 68,000, 27,000, and a low molecular weight peak (16,000). The 27,000 peak is identical in molecular weight to the myelin basic protein. The low molecular weight peak also co-runs with a myelin protein. (*B*) 10 d after injection. The pattern is similar to that of the injection site at 15 min, except that the prominent 68,000 peak is completely absent from the injection site.

sion? Two observations argue in favor of axonal transport. First, the distribution of labeled proteins found (e.g., after 10 d, Fig. 2) cannot be explained by diffusion. Second, analysis of SDS gel patterns of labeled proteins, described in detail below, shows that there is selective movement of different proteins at different rates, and that different labeled proteins are moving in the anterograde vs. retrograde direction.

Analysis of Labeled Proteins at the Injection Site

Proteins from the injection site were separated by SDS gel electrophoresis at 15 min after injection (0 h) and 10 d after injection of [^{3}H]*N*-SP. Fig. 4*A* shows the labeling profile on the gel immediately after injection. There is a diffuse distribution of label in the high molecular weight region of the gel, and three prominent peaks at 68,000, 27,000, and 16,000 (the latter peak ran near to the gel front, and therefore we are less certain of this molecular weight value). This labeling profile is very similar to the Coomassie Blue staining pattern on the gel (unpublished data), and indicates that both neuronal and non-neuronal proteins in the sciatic nerve segment are being labeled.

FIGURE 3 Autoradiographs of injected sciatic nerves 5 and 10 d after subepineural injection of [^{3}H]*N*-SP. 7-μm sections were autoradiographed as described in Materials and Methods. (*A*) Low power view. The injection site (asterisk) shows diffuse label of all neural elements. Extending from the injection site, the label is confined to a linear pattern, consistent with axonal location of the transported label. The patterns both proximal and distal to the injection site at 5 and 10 d were identical. Bar, 0.2 mm. (*B*) Cross-sectional view of retrograde direction at 10 d. Label is seen to be confined principally to the axons. Bar, 50 μm. (*C*) Cross-sectional view, anterograde direction at 5 d. Note that silver grains are in axons, surrounded by unlabeled myelin. Blood vessel (arrow) is largely unlabeled. Bar, 25 μm. (*D*) Longitudinal section, 10 d. Again, label is confined to center of axons. Myelin and Schwann cell nuclei (arrow) are unlabeled. Bar, 25 μm.

In fact, the 27,000 and 16,000 peaks correspond to the major protein components identified by Coomassie Blue staining which fractionate with myelin in rat sciatic nerve (20, 34). The 68,000 peak is also characteristic of sciatic nerve (32, 39, 41).

5–10 d after the injection, the gels of the injection site (Fig. 4 *B*) show a general decrease in overall radioactivity but persistence of the label in the major peaks at 27,000 and 16,000. However, the 68,000 peak was completely absent. The general persistence of labeled proteins for as long as 10 d implies that the labeled proteins at the injection site have an appreciable half-life. Similar experiments were also done 5 d after injection, and the data obtained were not significantly different from the 10-d data shown in Fig. 4 *B*. The persistence of the 27,000 and 16,000 peaks at the injection site might be expected, as myelin is confined to the Schwann cell and would not be expected to migrate within the nerve. The specific loss of the 68,000 peak indicates either that it has a rapid turnover or that it may have been transported out of the injection site. If the latter is the case, one would expect to find it in other segments of the nerve at later time points.

Analysis of Labeled Proteins Transported in the Anterograde Direction

The gel labeling profiles of several segments in the anterograde direction at 5 d after injection are shown in Fig. 5. Protein patterns from 3-mm segments that were 8, 20, and 26 mm from the injection site are shown in Fig. 5 *A*, *B*, and *C*, respectively. If the proteins move continuously at average velocities, then proteins that had moved these distances would correspond to average speeds of 1.6, 4, and >5 mm/d.

First inspection of the patterns makes two important facts obvious. The patterns are clearly different from the pattern of labeled proteins at the injection site. Thus the transported proteins represent a specific subset of all labeled proteins and not a random diffusion of either label or protein from the injection site. Second, the patterns vary from segment to segment, in agreement with previous work using other paradigms in which the nature of the proteins transported has varied according to the velocity at which they are transported (49).

At 8 mm from the injection site (Fig. 5 *A*), the principal peaks are at >200,000 (near the gel origin), 165,000, 140,000, 75,000, a doublet at 57,000–55,000, as well as complex peaks at 35,000–45,000 and 20,000–30,000, with a large peak of low molecular weight protein at the gel front. In terms of recognizable components, the proteins at >200,000, 165,000, and 68,000 may correspond to the neurofilament triplet and the 57,000–55,000 doublet to tubulin which has been shown by Hoffman and Lasek (22, 30) to move in the Sc_a component of slow transport at ~1 mm/d in this system.

The gel profile obtained from the segment 20 mm from the origin (Fig. 5 *B*), corresponding to an average rate of 4 mm/d, shows a predominant peak at 55,000. Except for the dominance of the 55,000 peak and a low molecular weight peak, it was not possible to analyze this complex pattern and compare it to previous reports in the literature. These proteins may be related to the complex Sc_b component of slow transport which has been described by Lasek and Hoffman in this system to move at an average rate of 2–4 mm/d (22, 30). The data at 26 mm from the injection site at 5 d (Fig. 5 *C*) also show a complex pattern, different from that of the 8- and 20-mm segments described above. These proteins may be related to the intermediate components, moving at >5 mm a day, i.e., at rates intermediate between slow and fast transport. Despite the complexity of the gel labeling profiles, it is clear that there is differential transport of the various labeled proteins which have moved out of the injection site.

To better resolve the selective nature of the transport, we evaluated gel labeling patterns in nerves 10 d after injection. At that time, proteins which have moved 8, 14, and 20 mm correspond to average velocities of 0.8, 1.4, and 2.0 mm/d, respectively. At this later time point, the components moving at 1 mm/d might separate from those moving at 2 mm/d more clearly (i.e., Sc_a and Sc_b, respectively). The results are shown in Fig. 6. The pattern of the slowest moving component (Fig. 6 *A*). The pattern seen in Fig. 6 *B* (representing the 1.4 mm/d component) differs from that of Fig. 6 *A* mostly in peak heights and is similar to the Sc_a slow component of Lasek and Hoffman (22, 30), with very clear peaks at >200,000 (near gel origin), 160,000, 145,000, and 68,000. The gel profile seen at 20 mm in 10 d (Fig. 6 *C*) differs from the previous two. The three sets of data all together reinforce the view of selective transport.

These types of experiments can also address the question of the coherence of a particular transport

component. For example, we have seen that the Sc_a slow component is well represented at 1.4 mm/d (Fig. 6 *B*) and at 0.8 mm/d (Fig. 6 *A*). If one now waits longer times after injection, e.g., for 45 d, one still finds significant amounts of labeled protein in anterograde segments within 20 mm of the injection site. Fig. 7 shows a gel profile of one of these segments, i.e., corresponding to an average movement of 0.38 mm/d. This profile is also characteristic of Sc_a proteins. At the time of injection, virtually all of the label was confined to about a 15-mm length of the sciatic nerve. If all the Sc_a proteins moved at exactly 1.4 mm/d, one would still expect the total length occupied by these proteins to be 15 mm. We have found that in 45 d when the Sc_a proteins at the center of the injection site should have been 63 mm down the axon, there were still Sc_a proteins as close as 12 mm from the injection site, i.e., the Sc_a proteins now range over a distance of at least double their original distance.

Analysis of Labeled Proteins Transported in the Retrograde Direction

The pattern of labeled proteins moving in the retrograde direction is shown in Fig. 8. In contrast to the complex patterns moving slowly in the anterograde direction, there is one major peak moving in the retrograde direction with an appar-

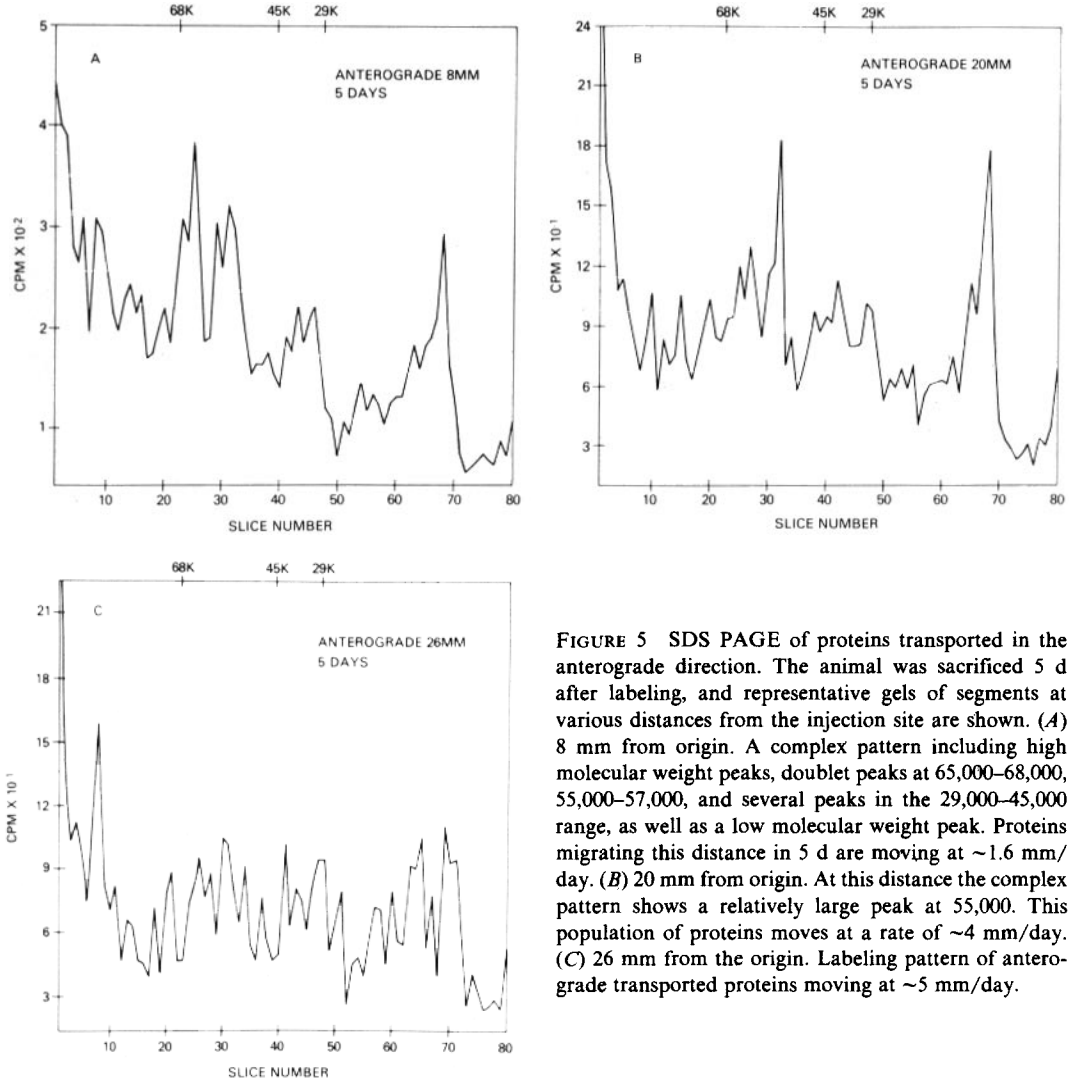

FIGURE 5 SDS PAGE of proteins transported in the anterograde direction. The animal was sacrificed 5 d after labeling, and representative gels of segments at various distances from the injection site are shown. (*A*) 8 mm from origin. A complex pattern including high molecular weight peaks, doublet peaks at 65,000–68,000, 55,000–57,000, and several peaks in the 29,000–45,000 range, as well as a low molecular weight peak. Proteins migrating this distance in 5 d are moving at ~1.6 mm/day. (*B*) 20 mm from origin. At this distance the complex pattern shows a relatively large peak at 55,000. This population of proteins moves at a rate of ~4 mm/day. (*C*) 26 mm from the origin. Labeling pattern of anterograde transported proteins moving at ~5 mm/day.

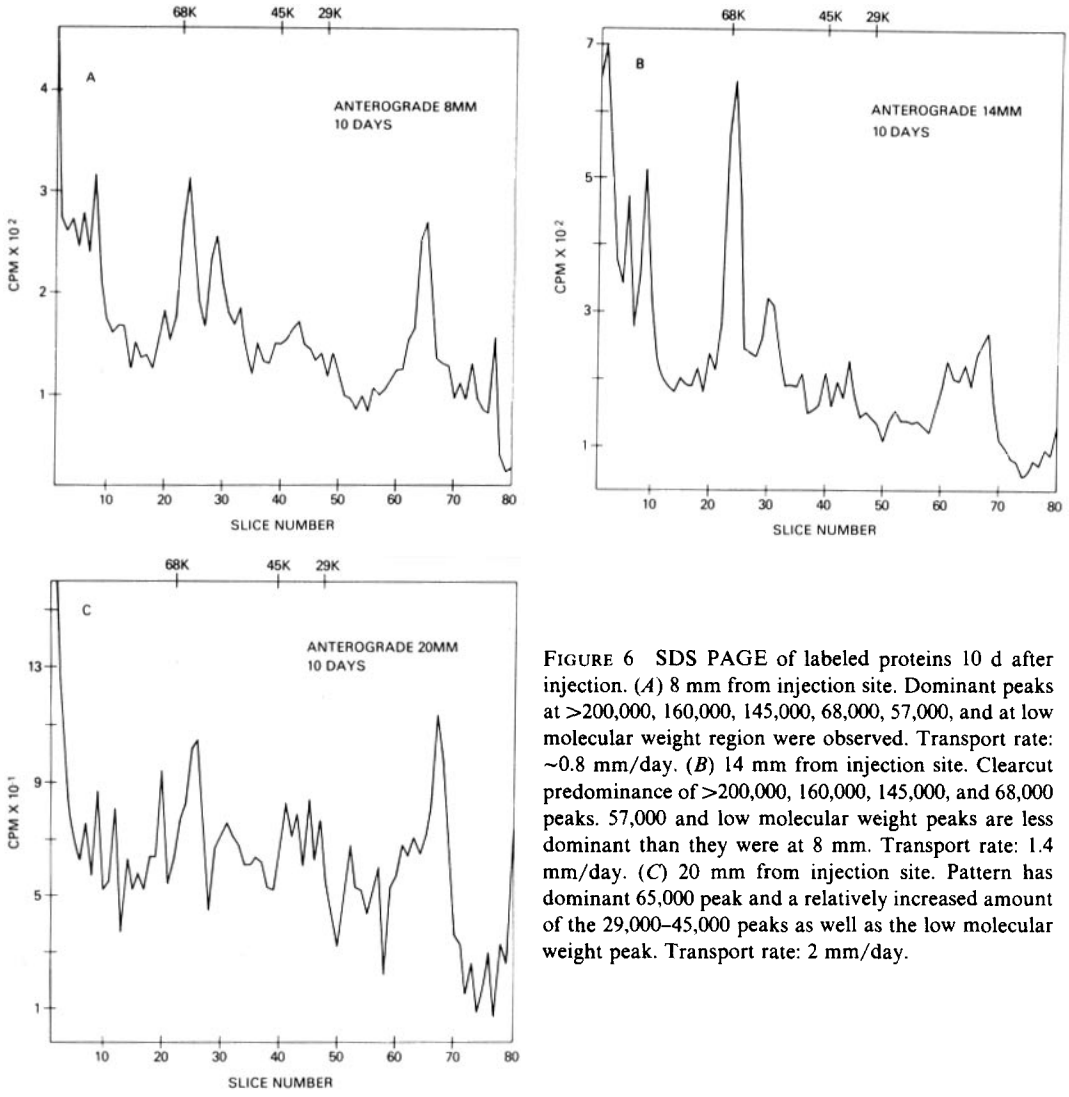

FIGURE 6 SDS PAGE of labeled proteins 10 d after injection. (*A*) 8 mm from injection site. Dominant peaks at >200,000, 160,000, 145,000, 68,000, 57,000, and at low molecular weight region were observed. Transport rate: ~0.8 mm/day. (*B*) 14 mm from injection site. Clearcut predominance of >200,000, 160,000, 145,000, and 68,000 peaks. 57,000 and low molecular weight peaks are less dominant than they were at 8 mm. Transport rate: 1.4 mm/day. (*C*) 20 mm from injection site. Pattern has dominant 65,000 peak and a relatively increased amount of the 29,000–45,000 peaks as well as the low molecular weight peak. Transport rate: 2 mm/day.

ent mol wt of 68,000. There are smaller peaks at 55,000 and 57,000 as well as a variable amount of lower molecular weight protein transported in the retrograde direction, but the vast majority of the counts are found in the 68,000 peak. This peak corresponds in size to the very large 68,000 peak at the origin, which specifically disappears from the injection site at 5 and 10 d after the injection (Fig. 4).

Fig. 9 shows a slab gel autoradiogram of the injection site and three segments, 8, 14, and 20 mm from the injection site in the retrograde direction 10 d after injection. The pattern of the injection site differs in that it does not contain the 68,000 peak which is prominent in all the segments and the 27,000 and 16,000 proteins are present only in the injection site. Furthermore, unlike the anterograde transport system, the retrograde system does not appear to move proteins differentially. Each of the segments is identical in labeling profile. As was pointed out earlier, this retrograde component does not appear to be transported all the way to the cell body (i.e., sensory ganglion or spinal cord) but appears to decrease in radioactivity, en route, after a few days.

Rapidly Transported Proteins

We were not successful in producing an early

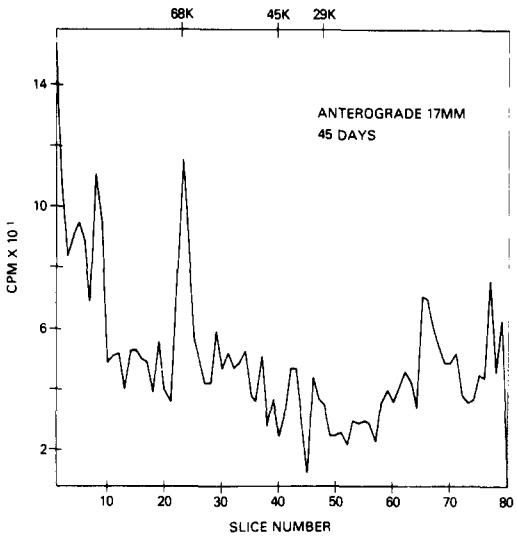

FIGURE 7 SDS PAGE of labeled proteins in the anterograde direction, 45 d after injection and 17 mm from the injection site. Pattern shows predominance of 160,000, 145,000, and 68,000 peaks.

discrete wave of activity in the sciatic nerve by the [^{3}H]*N*-SP method, which would be comparable to the fast component of axonal transport found with pulse-labeling methods (18, 29, 37). However, by injecting four times the amount of [^{3}H]*N*-SP injected, and taking segments 12 mm from the injected site 1 h later (i.e., on the exponentially falling part of the curve in both the anterograde and retrograde directions which had ~10,000–12,000 cpm/segment), it was possible to get SDS gel patterns of the fast-transported proteins (Fig. 10). The patterns observed were very complex. They are clearly different from the injection site but also differ from the slowly transported retrograde and anterograde proteins.

DISCUSSION

Ever since the discovery of axonal transport by the classic work of Weiss and Hiscoe (48), diverse approaches and methods have been employed which have altered our view of this intracellular process in neurons. One of the most valuable of these has been the utilization of radioactive amino acids in a pulse-label paradigm, to demonstrate the fast axonal transport component (18, 29, 37). With this approach it has been possible to show that there are discrete constellations of proteins being transported intra-axonally at rates ranging from <0.5 mm/d to ~500 mm/d from the nerve cell body towards the nerve terminal (18, 22–24, 29, 30, 33, 37, 44, 49–51). Furthermore, this approach has provided information about neuronal organization, e.g., fast transport appears to move membrane-bound proteins (18, 30), whereas slow transport moves cytoskeletal proteins (22, 30).

Others have utilized the enzyme activity of intra-axonal proteins to study axonal transport. Various enzymes activities increase on both the proximal and distal sides of a ligature or cold block (5, 6, 9, 10, 12, 13, 15, 25, 27, 38, 52). Calculation of the rate of accumulation allows the average rate of transport of these enzymes to be measured (9, 47). This accumulation of activity on both sides of the ligature implies bidirectional movement of these enzymes. After release of the cold block a peak of activity can be followed moving proximodistally down the axon (5, 6). In those cases where cold block has been used, the velocity of transport calculated on the basis of the accumulation is less than the maximum velocity seen when the cold block is released (47). This has been interpreted as indicating that a substantial percentage of the axonal enzyme is stationary at any given time. For 3,4-dihydroxyphenylalanine decarboxylase, Starkey and Brimijoin (47) have es-

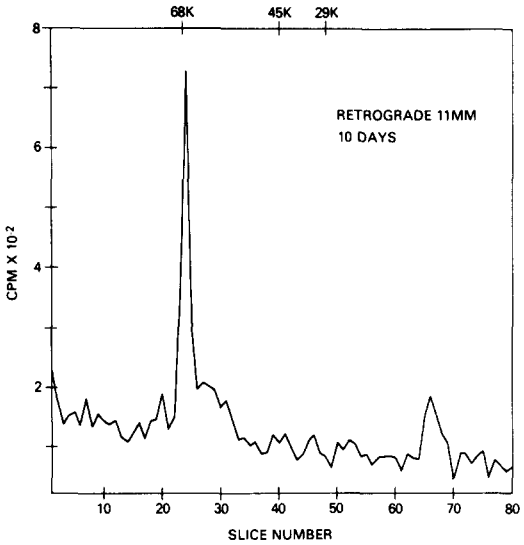

FIGURE 8 SDS PAGE of labeled proteins transported in retrograde direction, towards neuronal perikaryon, 10 d after injection. This labeling pattern is dramatically different than that in the anterograde direction (see Fig. 6*A*) and appears to be composed primarily of the 68,000 peak. Note that the predominant labeled peak in the injection site that disappeared after 10 d was 68,000 (see Figs. 4*A* and 9).

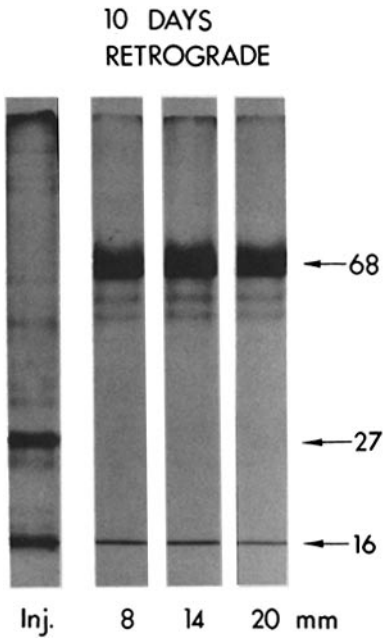

FIGURE 9 Fluorograph of SDS slab gel containing labeled proteins transported in retrograde direction 10 d after injection of isotope. Figure shows injection site and three segments in retrograde direction 8, 14, and 20 mm from injection site. An equal number of counts was applied in each sample. All the retrograde segments appear to have identical protein compositions. The 68,000 peak appears to move at a relatively slow rate of ~3 mm/d.

timated that as little as 15% of the enzyme in the axon may be undergoing axonal transport at any given time.

Direct light microscope observation of axons in vitro allows direct visualization of the movement of intra-axonal particles (8, 11, 26). These particles appear to undergo discontinuous saltatory motion in both directions, with 90% of the particles showing a predominant retrograde direction (11).

The picture of axonal transport which emerges from each of these studies, in large part, reflects the nature of the method used to obtain it. Pulse-label studies focus on newly synthesized neuronal proteins and are therefore limited to proximodistal transport. These emphasize wavelike movements. Redistribution of enzyme activity is limited to those proteins with assayable activity, and must be studied in a pathologic condition of ligature or cold block. This approach reveals the presence of stationary components in the axon. Direct observation, limited to particles visible by light microscopy, focuses upon the predominant retrograde transport of particles in that size class.

In this study we have used a new covalent labeling method to label intra-axonal proteins in

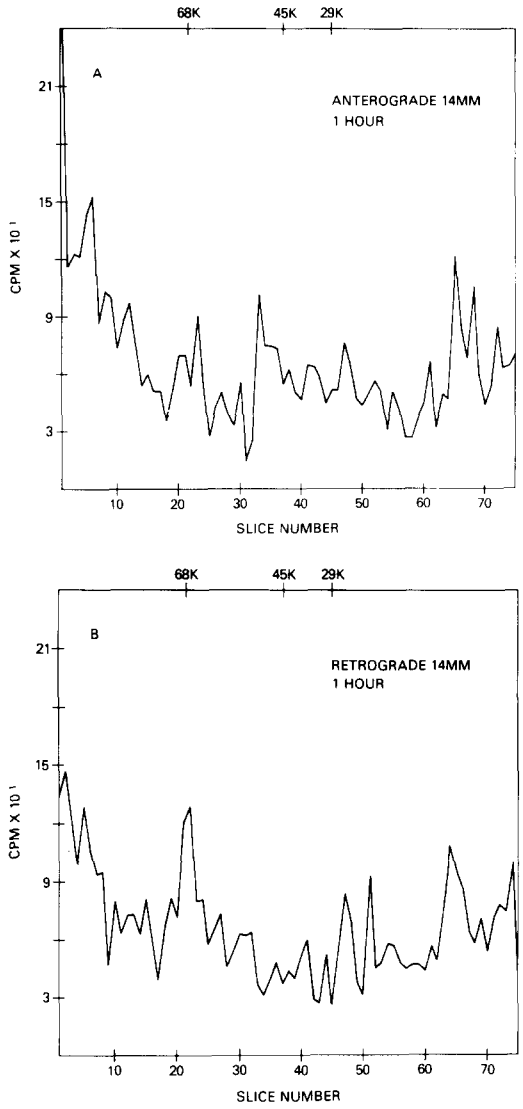

FIGURE 10 11% SDS PAGE of labeled proteins transported in rapid phase of axonal transport. 400 μCi of [^{3}H]*N*-SP was injected into the sciatic nerve, and the segments 14 mm on either side of the injection site were collected after 1 h. (*A*) Labeling pattern in the anterograde direction. (*B*) Labeling pattern in the retrograde direction. Note that a significant 68,000 peak appears in the retrograde direction even after only 1 h. The amount of [^{3}H]*N*-SP labeled protein which moves rapidly is only a small fraction of the labeled proteins which move at the slower rates.

vivo. Because the proteins are labeled in the axon, independent of their synthesis, a unique view of the intra-axonal movement of proteins in an unperturbed nerve is obtained. Most of our experimental observations regarding anterograde axonal transport were on the slow and intermediate rates, as most of the labeled intra-axonal proteins were in these components. Using [^{3}H]*N*-SP covalent labeling of axonal proteins, we have confirmed the previous reports of multiple waves of transport (36, 49–51) and have shown that the slow component of transport is formed by two separate components, i.e., the Sc_a and Sc_b components described by Lasek and Hoffman (22, 30). These data suggest that the [^{3}H]*N*-SP labeling paradigm did not disrupt the normal axonal transport processes.

Our inability to extensively study the fast axonal transport mechanism by the [^{3}H]*N*-SP method may reflect the small absolute amount of proteins in this component in the sciatic nerve. These proteins turn over very rapidly and are probably best studied by the traditional pulse-labeling paradigm. Despite this difficulty, our data suggest that the rapidly transported proteins are very similar in the anterograde and retrograde directions, again in agreement with previous reports (1, 4). However, we have succeeded in studying fast axonal transport by the [^{3}H]*N*-SP method, in the hypothalamo-neurohypophysial system (manuscript in preparation). The reason that the method is effective in the neurosecretory system is probably because a relatively large amount of neurosecretory proteins is being transported in this component (14).

The most significant new finding in this study is that we have observed a selective movement of proteins in the retrograde direction (Figs. 8 and 9), moving at ~3–6 mm/d. This retrograde component is composed primarily of a very large 68,000 peak, probably the same as the one seen at the injection site initially, which then completely disappears by 5–10 d (Fig. 2). A protein of similar size (68,000) has been reported as an abundant component in a neurofilament preparation from rat sciatic nerve (39, 41). It has been suggested that this 68,000 protein may represent principally a serum albumin contaminant of the extract (32). However, our 68,000 peak is found exclusively intra-axonally and is transported principally in the retrograde direction. If it is serum albumin, then it is found intracellularly. In this regard, it is interesting that immunocytochemical evidence for the intracellular localization of serum proteins in neurons with projections to the periphery has recently been reported (46).

Covalent labeling agents have traditionally been used to determine whether proteins on the cell plasma membrane are located on the cytoplasmic or the extracellular surface (7). In this work, we have shown that extracellularly applied covalent-labeling agents can label intracellular proteins as well, with no obvious deleterious effects on cell function. [^{3}H]*N*-SP and other similar reagents may, therefore, be able to serve as radioactive "supra-vital stains" in various cell biological and neurobiological experimental paradigms. This type of "stain" has an added feature, in that it allows for the study of the dynamic behavior of specific intracellular proteins.

We wish to thank Dr. Elaine Neale for assistance with the autoradiography and Chris Merritt for his technical assistance.

Received for publication 25 June 1979, and in revised form 7 January 1980.

REFERENCES

1. ABE, T., T. HAGA, and M. KUROKAWA. 1974. Retrograde axonal transport: Its continuation as anterograde transport. *FEBS (Fed. Eur. Biochem. Soc.) Lett.* **47**:272–278.
2. BONNER, W. M., and R. A. LASKEY. 1974. A film detection method for tritium labeled proteins and nucleic acids in polyacrylamide gels. *Eur. J. Biochem.* **46**:83–88.
3. BOYD, H., I. C. CALDER, S. J. LEACH, and B. MILLIGAN. 1972. N-acylsuccinimides as acylating agents for proteins: Synthesis, hydrolysis and aminolysis. *Int. J. Pept. Prot. Res.* **4**:109–115.
4. BRAY, J., C. KON, and B. BRECKENRIDGE. 1971. Reversed polarity of rapid axonal transport in chicken motoneuron. *Brain Res.* **33**:560–564.
5. BRIMIJOIN, S. 1975. Stop-flow: A new technique for measuring axonal transport, and its application to the transport of dopamine-β-hydroxylase. *J. Neurobiol.* **6**:379–394.
6. BRIMIJOIN, S., and M. J. WIERMAA. 1977. Direct comparison of the rapid axonal transport of norepinephrine and dopamine-β-hydroxylase activity. *J. Neurobiol.* **8**:239–250.
7. CARRAWAY, K. L. 1975. Covalent labeling of membranes. *Biochim. Biophys. Acta.* **415**:379–410.
8. COOPER, P., and R. SMITH. 1974. The movement of optically detectable organelles in myelinated axons of *Xenopus laevis*. *J. Physiol. (Lond.).* **242**:77–97.
9. COYLE, J. T., and G. F. WOOTEN. 1972. Rapid axonal transport of tyrosine hydroxylase and dopamine-β-hydroxylase. *Brain Res.* **44**:701–704.
10. DAHLSTROM, A., and J. HAGGENDAL. 1966. Studies on the transport and lifespan of amine storage granules in a peripheral adrenergic neuron system. *Acta Physiol. Scand.* **67**:278–288.
11. FOREMAN, D., P. PADJEN, AND G. SIGGENS. 1977. Axonal transport of organelles visualized by light nicroscopy. *Brain Res.* **136**:197–213.
12. FRIZELL, M., W. M. MCLEAN, and J. SJOSTRAND. 1970. Retrograde axonal transport of rapidly migrating labeled proteins and glycoproteins in regenerating peripheral nerves. *J. Neurochem.* **27**:191–196.
13. FRIZELL, M., P. HASSELGREN, AND J. SJOSTRAND. 1970. Axoplasmic transport of acetylcholinesterase and choline acetyltransferase in the vagus and hypoglossal nerve of the rabbit. *Exp. Brain Res.* **10**:526–531.
14. GAINER, H., Y. SARNE, AND M. J. BROWNSTEIN. 1977. Biosynthesis and axonal transport of rat neurohypophysial proteins and peptides. *J. Cell Biol.* **73**:366–381.
15. GEFFEN, L., and R. RUSH. 1968. Transport of noradrenaline in sympathetic nerves and the effect of nerve impulses on its contribution to transmitter stores. *J. Neurochem.* **15**:925–930.
16. GILBERT, D. S., B. J. NEWBY, and B. H. ANDERSON. 1975. Neurofilament disguise, destruction, and discipline. *Nature (Lond.).* **256**:586–589.

17. GRAFSTEIN, B. 1975. Principles of anterograde axonal transport in relation to studies of neuronal connectivity. *In* The Use of Axonal Transport for Studies of Neuronal Connectivity. W. Cowan and M. Cuenod, editors. Elsevier, Amsterdam. 47–65.
18. GRAFSTEIN, B. 1977. Axonal transport: The intracellular traffic of the neuron. *In* Handbook of Physiology: The Nervous System. I. J. Brookhart, V. Mountcastle, E. Kanael, editors. American Physiological Society, Bethesda, Md. 691–717.
19. GRAFSTEIN, B., B. S. MCEWEN, and M. L. SHELANSKI. 1970. Axonal transport of neurotubule protein. *Nature (Lond.).* **227:**289–290.
20. GREENFIELD, S., S. BROSTOFF, E. H. EYLAN, AND P. MORELL. 1973. Protein composition of myelin of the peripheral nervous system. *J. Neurochem.* **20:**1207–1216.
21. GRIFFIN, J., D. PRICE, D. DRACHMAN, and W. ENGEL. 1976. Axonal transport to and from the motor nerve ending. *Ann. N. Y. Acad. Sci.* **274:**31–45.
22. HOFFMAN, P. N., and R. J. LASEK. 1975. The slow component of axonal transport. *J. Cell Biol.* **66:**351–366.
23. JAMES, K., J. BRAY, I. MORGAN, and L. AUSTIN. 1970. The effect of colchicine on the transport of axonal protein in the chicken. *Biochem. J.* **117:**767–771.
24. KARLSSON, J.-O., and J. SJOSTRAND. 1971. Synthesis, migration and turnover of proteins in retinal ganglion cells. *J. Neurochem.* **18:**749–767.
25. KAPELLER, K., and D. MAYOR. 1967. The accumulation of noradrenaline in constricted sympathetic nerves as studied by fluorescence and electron microscopy. *Proc. Roy. Soc. London Ser. B.* **167:**282–292.
26. KIRKPATRICK, J., J. BRAY, and S. PALMER. 1972. Visualization of axoplasmic flow *in vitro* by Nomarski microscopy. Comparison to rapid flow of radioactive proteins. *Brain Res.* **43:**1–10.
27. JARROT, B., and L. B. GEFFEN. 1972. Rapid axoplasmic transport of tyrosine hydroxylase in relation to other cytoplasmic constituents. *Proc. Natl. Acad. Sci. U. S. A.* **69:**3440–3442.
28. LASEK, R. J. 1967. Bidirectional transport of radioactively labeled axoplasmic components. *Nature (Lond.).* **216:**1212–1214.
29. LASEK, R. J. 1970. Protein transport in neurons. *Int. Rev. Neurobiol.* **13:** 289–321.
30. LASEK, R. J., and P. N. HOFFMAN. 1976. The neuronal cytoskeleton, axonal transport and axonal growth. *In* Cell Motility. R. Goldman, T. Pollard, and J. Rosenbaum, editors. Cold Spring Harbor Laboratory, Cold Spring Harbor, N. Y. 1021–1049.
31. LEACH, S. J., and H. BOYD. 1973. Thermal transitions of acylated ribonuclease. *Int. J. Pept. Prot. Res.* **5:**239–250.
32. LIEM, R. K. H., Y. SHU-HUI, G. D. SALOMON, and M. L. SHELANSKI. 1978. Intermediate filaments in nervous tissues. *J. Cell Biol.* **79:**637–645.
33. MCGREGOR, A., Y. KOMIYA, A. KIDMAN, and L. AUSTIN. 1973. The blockage of axoplasmic flow of proteins by colchicine and cytochalasins A and B. *J. Neurochem.* **21:**1059–1066.
34. MICKO, S., and W. SCHLAEPFER. 1978. Protein composition of axons and myelin from rat and human peripheral nerves. *J. Neurochem.* **30:** 1044–1049.
35. NEVILLE, D. 1971. Molecular weight determination of protein-dodecyl sulfate complexes by gel electrophoresis in a discontinuous buffer system. *J. Biol. Chem.* **246:**6328–6334.
36. LORENZ, T., and M. WILLARD. 1978. Subcellular fractionation of intraaxonally transported polypeptides in the rabbit visual system. *Proc. Natl. Acad. Sci. U. S. A.* **75:**505–509.
37. OCHS, S. 1972. Fast transport of materials in mammalian nerve fibers. *Science (Wash. D. C.).* **176:**252–260.
38. RANISH, N., and S. OCHS. 1972. Fast axoplasmic transport of acetylcholinesterase in mammalian nerve fibers. *J. Neurochem.* **19:**2641–2649.
39. SCHLAEPFER, W. W. 1977. Immunological and ultrastructural studies of neurofilaments isolated from rat peripheral nerve. *J. Cell Biol.* **74:**226–240.
40. SCHLAEPFER, W. W., AND L. A. FREEMAN. 1978. Neurofilament proteins of rat peripheral nerve and spinal cord. *J. Cell Biol.* **78:**653–662.
41. SCHLAEPFER, W. W., and R. G. LYNCH. 1977. Immunofluorescence studies of neurofilaments in the rat and human peripheral and central nervous system. *J. Cell Biol.* **74:**241–250.
42. SCHLAEPFER, W., and S. MICKO. 1978. Chemical and structural changes of neurofilaments in transected rat sciatic nerve. *J. Cell Biol.* **78:**369–378.
43. SCHLAEPFER, W., and S. MICKO. 1979. Calcium-dependent alterations of neurofilament proteins of rat peripheral nerve. *J. Neurochem.* **32:** 211–219.
44. SCHWARTZ, J. H. 1979. Axonal transport: Components, mechanisms and specificity. *Annu. Rev. Neurosci.* **2:**467–504.
45. SMITH, R. 1971. Centripetal movement of particles in myelinated axon. *Cytobios.* **3:**259–262.
46. SPARROW, J. R., and J. A. KIESNAN. 1979. Immunocytochemical localization of plasma proteins in neuronal perikarya. *Soc. Neurosci.* **5:**63 (Abstr.).
47. STARKEY, R., and S. BRIMIJOIN. 1979. Stop-flow analysis of the axonal transport of DOPA decarboxylase in rabbit sciatic nerves. *J. Neurochem.* **32:**437–441.
48. WEISS, P. A., and H. HISCOE. 1948. Experiments on the mechanism of nerve growth. *J. Exp. Zool.* **107:**315–395.
49. WILLARD, M., W. COWAN, AND P. VAGELOS. 1974. The polypeptide composition of intraaxonally transported proteins: Evidence for four transport velocities. *Proc. Natl. Acad. Sci. U. S. A.* **71:** 2183–2187.
50. WILLARD, M. 1977. The identification of two intra-axonally transported polypeptides resembling myosin in some respects in the rabbit visual system. *J. Cell Biol.* **75:**1–11.
51. WILLARD, M., and E. HULEBECK. 1977. The intraaxonal transport of polypeptide H: Evidence for a fifth (very slow) group of transported proteins. *Brain Res.* **136:**277–288.
52. ZELENA, S., L. LUBINSKA, and E. GUTMANN. 1968. Accumulation of organelles at the ends of interrupted axons. *Z. Zellforsch. Mikrosk. Anat.* **91:**200–219.